Pure Leptonic Decays of the D and D_s Mesons[†]

Peter C. Kim

Stanford Linear Accelerator Center,

Stanford University, Stanford, CA

Abstract

This report presents a feasibility study of the pure leptonic decays of charmed mesons at a Tau-Charm Factory. A year of running with a luminosity of $10^{33}\ cm^{-2}sec^{-1}$ would allow precise measurement of f_D and f_{D_s} at a percent level, providing a benchmark test of Lattice QCD calculations. Possible observation of mass-dependent couplings in D_s decays to $\tau\nu$ and $\mu\nu$ is also discussed.

INTRODUCTION

Pure leptonic decays are the simplest weak decays involving the charmed mesons (Fig.1). In principle, these decay rates can be well predicted by the Standard Model of the electroweak interaction. Only the axial vector component of the hadronic charged current contributes to the leptonic decays of a pseudoscalar meson,[1]

$$< 0 \mid J_\alpha^\dagger \mid D^+ >= iq_\alpha V_{cd} f_D$$

where $J_\alpha^\dagger$ is the axial vector current, q_α the momentum transfer, V_{cd} the K-M matrix element, and f_D the weak decay constant of D meson, which is a parameter describing

† **This work was supported in part by the U. S. Department of Energy, under contracts DE-AC03-76SF00515**

the effect of strong interaction on the charm meson-W coupling. In a nonrelativistic quark model, the weak decay constant is proportional to the wavefunction overlap of the constituent quarks ($c\bar{q}$) inside the charm meson:

$$f_D^2 \propto \frac{|\Psi(0)|^2}{m_D}$$

where $\Psi(0)$ is the wavefunction at the origin. The quark-antiquark annihilation is expected to occur inside an average distance of $r = 1/m_D$.

The decay probability of the leptonic decay is

$$\Gamma(D^+ \to l^+\nu) = \frac{G_F^2}{8\pi} f_D^2 \, m_D \, m_l^2 \, |V_{cd}|^2 \left(1 - \frac{m_l^2}{m_D^2}\right)^2$$

where G_F is the Fermi coupling constant, m_l the lepton mass, and m_D the mass of D meson. Due to the V-A nature of weak interaction, it is helicity-suppressed. In other words, the decay width is dependent on the lepton mass in the final state, and it vanishes in the limit $m_l \to 0$. By measuring the branching fraction, combined with the knowledge of V_{cd} and the D meson lifetime, we could determine the weak decay constant of the D mesons.

Table I. Leptonic Branching Fractions and f_D

f_D or f_{Ds} [MeV]	$B(D^+ \to \mu^+\nu)$	$B(D_s^+ \to \mu^+\nu)$	$B(D_s^+ \to \tau^+\nu)$
150	2.0×10^{-4}	1.7×10^{-3}	0.9×10^{-2}
175	2.7×10^{-4}	2.3×10^{-3}	1.2×10^{-2}
200	3.5×10^{-4}	3.0×10^{-3}	1.5×10^{-2}
225	4.5×10^{-4}	3.8×10^{-3}	1.9×10^{-2}
250	5.5×10^{-4}	4.8×10^{-3}	2.4×10^{-2}

Table I shows the branching fractions of the leptonic decays for different values of f_D and f_{Ds}. At present, there exists no experimental observation of the leptonic decays, only an upper limit of 290 MeV from the MARK III Collaboration.[2] For this study, we have used $f_D = 175$ MeV and $f_{Ds} = 225$ MeV.

Table II. Theoretical Estimates of Weak Decay Constants

Author	Year	Type	f_D	f_{Ds}	f_{Bd}	f_B/f_D
Mathur and Yamawaki	(81)	QCD SUM RULE	192	232	241	1.3
Aliev and Eletskii	(83)	QCD SUM RULE	170	-	132	0.8
Shifman	(87)	QCD SUM RULE	170	-	110/130	0.7/0.8
Narison	(87)	QCD SUM RULE	173	-	187	1.1
Dominguez and Paver	(87)	QCD SUM RULE	220	270	140/210	0.6/1.0
Reinders	(88)	QCD SUM RULE	170	-	132	0.8
Kraseman	(80)	POTENTIAL	150	210	125	0.8
Suzuki	(85)	POTENTIAL	138	-	89	0.6
Godfrey and Isgur	(85-86)	POTENTIAL	234	391	191	0.8
Bernard	(88)	LATTICE	174	234	105	0.6
DeGrand and Loft	(88)	LATTICE	134	157	-	-
Golowich	(80)	BAG	147	166	-	-

There are basically three different types of theoretical models in calculating the weak decay constant: Potential and Bag model, QCD sum rules, and Lattice QCD model. Various theoretical estimates can be found in Table II.[3] Predicted values vary greatly, even between models following a similar approach, but interestingly, the ratio of f_B/f_D comes out to be similar to one another. Hence, with precise measurement of f_D and f_{D_s}, f_B can be extrapolated reliably. Direct experimental measurement of f_B in $B^+ \to \tau^+\nu$ decay is expected to be very difficult, due to the small value of the K-M matrix element, V_{ub}.

The weak decay constant is one of the easier values to calculate in a Lattice QCD model, and ultimately, Lattice calculations will provide the best theoretical estimate for f_D. Or conversely, if f_D is well-measured experimentally, it can be used to test the Lattice QCD models.

By measuring the decay widths of both $D_s^+ \to \mu^+\nu$ and $D_s^+ \to \tau^+\nu$, we can also test the lepton universality and V-A structure of weak interaction, or search for new effects beyond the Standard Model. One could also look for the charged Higgs contribution,

since the Higgs-fermion coupling is mass-dependent.

Existing upper limit on charged Higgs from the JADE collaboration[4] rules out the mass range, $4.0 < m_{H^+} < 15$ GeV, and present data on τ decay[5] rules out $m_{H^+} < m_\tau$. Therefore, there is a small opening of 2–4 GeV region for a charged Higgs, which could enhance the $\tau\nu$ rate over the $\mu\nu$ in the D_s decay. Since the mass region is above the charmed meson masses, charged Higgs bosons mediate the weak force as virtual particles similar to the usual W-propagator. Neglecting the strong-interaction corrections, we have[6]

$$\frac{\Gamma(D_s^+ \to H^+ \to l^+\nu)}{\Gamma(D_s^+ \to W^+ \to l^+\nu)} \simeq \frac{m_c^2 m_l^2}{(m_{H^+}^2 - m_{D_s^+}^2)^2}$$

where m_c is the charm quark mass. In fact, if the Higgs mass is close the D_s mass, $\tau\nu$ could be the most dominant decay channel. It is interesting to note that recent estimate of $B(D_s^+ \to \phi\pi^+) = 2.0 \pm 0.9\%$ from CLEO[7] indicates that there are a lot of branching fractions not yet accounted for in D_s decay.

The hadronic cross section, R, in e^+e^- annihilation will increase above the H^+H^- threshold by only 1/4 of a unit at the most, since the Higgs particles are scalars:[8]

$$R_{H^+H^-} = \frac{1}{4}\left[1 - \frac{4m_H^2}{s}\right]$$

This rise is very slow above threshold, and it is difficult to observe experimentally unless the Higgs particle decays mainly into hadrons. The above JADE limit comes from a study of acolinearity of the leptons from τ pairs in e^+e^- annihilation at $E_{cm} = 37$ GeV, assuming a certain branching fraction for $H^+ \to \tau^+\nu$. This method of using secondary τ-pairs is, however, insensitive for low mass Higgs close to τ mass. Hence, leptonic decay of the D_s could be the most strict test of the 2–4 GeV mass region. Effect of charged Higgs on τ decay is discussed in the paper by Y. Tsai in these proceedings.

Study of leptonic decay is rather straightforward at a Tau-Charm Factory, due to the simplicity of the $D\overline{D}$ production near threshold. Since the $\psi(3770)$ resonance decays to $D\overline{D}$ predominantly, by tagging a D^- in a event, we can be sure that the rest of the event comes from a D^+ decay. The situation is also similar for the case of $D_s^+D_s^-$ production at $E_{cm} = 4.03$ GeV, even though the charm cross section at this energy is dominated by $D^*\overline{D^*}$, $D\overline{D^*}$, and $D\overline{D}$ cross sections. At a Tau-Charm Factory, we expect a large number of tagged charm events:[9] 1.2×10^7 D^0, 5.5×10^6 D^+, and 8.3×10^5 D_s single tags, after 1 year of running with a luminosity of 10^{33} $cm^{-2}sec^{-1}$.

DETECTOR AND MONTE CARLO SIMULATION

For the study of leptonic decays, the most important features in the detector design are lepton identification and hermeticity of the whole detector. Lepton identification is achieved mainly with the calorimeter system, Electromagnetic (EM) calorimeter and Hadron tagger, by studying the shower shape and the range of shower depth. Since there are missing particles, one or more neutrinos, in the final state, hermeticity of the detector is crucial in suppressing the background. The solid angle coverage of the drift chamber is down to an angle of cosine less than 0.95. As for the calorimeter system, energy resolutions of the EM calorimeter or the Hadron tagger are not as important as the requirement for high efficiency in detecting neutral particles to reject background. This study employed a conventional EM calorimeter design with 8 % energy resolution. Good momentum resolution of the charged tracks will help the study of $D^+ \to \mu^+\nu$ and $D_s^+ \to \mu^+\nu$, providing narrow missing mass peaks, but not for the $D_s^+ \to \tau^+\nu$ decay where there is no clear distinction between the signal and background shapes. The performances of each detector components are stored in parametrized tables to facilitate background study with large numbers of events. A detailed description of the specification and performances of the designed detector can be found elsewhere.[10]

The Tau-Charm Monte Carlo used for this study is based on the Mark III event generators and D meson decay models. For the D_s decay, each decay channel is generated separately, since there exists no reliable decay model.

As for the tags, we have generated only the following two channels: $D^- \to K^+\pi^-\pi^-$ and $D_s^- \to \phi\pi^-$. Detection efficiencies are found against these tags, and then the expected numbers of observed leptonic events are determined by scaling the number of tags. It is true that these two channels give clean background-free tags, while other tag channels, especially the ones with photons, have substantial background under the signal. However, previous Mark III studies of leptonic and semileptonic decays against tags have shown that the background rate under the tag is unimportant, as it amounts a double-tagging of each event.[11]

ANALYSIS

The analysis procedure for the leptonic decay channels are as follows. First, 4-prong candidate events are selected, and it is reguired one of the charged track is identified as a lepton, while the rest as hadrons. Next, beam-constrained mass of the hadrons, defined as $M^2 = E_{beam}^2 - P^2$, is plotted to see whether they form either a D^+ or a D_s meson. Finally, we plot the square of the missing mass in each event,

$$(\text{Missing Mass})^2 = (E_{CM} - E_{obs})^2 - P_{obs}^2$$

The signal events show a narrow missing mass peak centered at zero for the $D^+ \to \mu^+\nu$ and $D_s^+ \to \mu^+\nu$ decays, and a broad distribution for the $D_s^+ \to \tau^+\nu$; $\tau^+ \to \mu^+(or\ e^+)\nu\bar{\nu}$ decay.

The charged tracks are selected by requiring $p_t > 20$ MeV and $|\ cos\theta\ | < 0.95$. Identification of the charged tracks relies on the TOF measurement. For each particle hypothesis, respective weight is calculated from the χ^2 of the difference between measured and calculated flight times. The track is identified as pion, if the pion weight is greater than that of a kaon, and *vice versa*. When no TOF information is available, the track is assigned as a pion.

The candidate events must have exactly 4 charged tracks with no other visible energy in the rest of the detector. To remove the photon background, no *isolated* energy

deposits greater than 30 MeV in the EM calorimeter are allowed. (*isolated* means there are no charged tracks within an angle of cosine greater than 0.95.) Furthermore, the K_L^0 background is eliminated by requring no *isolated* energy deposits greater than 30 MeV in the Hadronic tagger.

The D^- and D_s^- tags are selected by requiring the $K^+\pi^-\pi^-$ and $K^+K^-\pi^-$ beam-constrained masses to lie within 4 MeV and 2 MeV of the known charged D and D_s masses, respectively. An additional ϕ mass cut of $1.015 < M(K^+K^-) < 1.025$ GeV is applied for the D_s^- tag. The detector reconstruction efficiencies are 53 % for the $D^- \to K^+\pi^-\pi^-$ decay and 21 % for the $D_s^- \to \phi\pi^- \to K^+K^-\pi^-$ decay.

The lepton identification of the single track, not belonging to the tag, is as follows. Muons are identified using the information from the TOF counters, Drift Chamber, EM calorimeter, and the Hadron tagger. The TOF measurement must be coinsistent with the muon hypotheis. Secondary muons, such as the ones from the charged kaon decays, are rejected by looking for the kinks in the drift chamber. Since the muon is a minimum ionizing particle, the energy deposited in the EM calorimeter and Hadron tagger differ greatly from those of hadrons. Also, the range of shower depth in the Hadron tagger is used for rejecting hadron background. Electron identification utilizes mainly the shower shape in the EM calorimeter, and the TOF measurement for electrons with low momenta.

For $D^+ \to \mu^+\nu$ and $D_s^+ \to \mu^+\nu$, the muon momentum distribution has a narrow peak near 1.0 GeV, since they are 2-body decays and the charmed mesons are produced almost at rest; we make momentum cuts of $0.80 < p(\mu) < 1.10$ GeV for the D^+ and $0.80 < p(\mu) < 1.20$ GeV for the D_s. The (Missing Mass)^2 in each event, which has passed all of the above requirements, is plotted in Fig. 2(a) for $D^+ \to \mu^+\nu$ and Fig. 2(b) for $D_s^+ \to \mu^+\nu$. Clear signals at zero missing mass are evident; detection efficiency for the muon is 74 %. The low lying backgrounds are from misidentified hadronic events, such as $K_L^0\pi^+$ and $\pi^0\pi^+$, and the semi-muonic decays, $K_L^0\mu^+\nu$ and $\pi^0\mu^+\nu$. We expect about 1100 detected events in $D^+ \to \mu^+\nu$ 2000 in $D_s^+ \to \mu^+\nu$ per year of running.

The study of $D_s^+ \to \tau^+\nu$ decay is much more complicated by the τ decay. Here, we have used the decay channels: $\tau^+ \to \mu^+\nu_\mu\overline{\nu}_\tau$ and $\tau^+ \to e^+\nu_e\overline{\nu}_\tau$, resulting in final states with a single charged lepton plus three missing neutrinos. The signals in missing mass plots have broad distributions (Fig. 2(c) and Fig. 2(d)). Since the background distribution also has a similar shape, the amount of signal has to be extracted by background subtraction, which relies heavily on the model of D_s decay and detector performances. Unfortunately, at present there are only a few D_s decay channels observed. Instead of using a D_s decay model, we have generated 50,000 events each in 20 different decay channels with low charged and neutral multiplicities. Table III lists the decay channels which contribute most to the background. Other channels can be removed by use of the calorimeter and lepton identification.

Table III. Sources of background for $D_s^+ \to \tau^+\nu \to \mu^+\nu\overline{\nu}\nu$.

Decay Channel	BR (%)	N(EM only)	N(EM+HAD)
$\overline{K}^0K^+$	3.0	40.0	9.3
$\phi\mu^+\nu$	3.0	2.3	2.3
$\eta\mu^+\nu$	1.5	7.0	7.0
$\overline{K}^0\mu^+\nu$	0.2	310	8.0
$\mu^+\nu$	0.4	2080	2000

Semi-leptonic decays with appropriate leptons are the main sources of background, while the $D_s^+ \to \mu^+\nu$ decay shows up as a spike at zero missing mass. The hadronic decay channels turn out to be not a major factor, as one of their charged tracks has to be misidentified as a lepton and also the rest of the charged and neutral tracks must escape detection. Importance of Hadron tagger can be seen by the improvement in background rate by a factor of four for the channels with a K_L^0, as shown in Fig. 3(a) and 3(b). Detector efficiencies are 67 % and 80 % for $\mu^+\nu\overline{\nu}\nu$ and $e^+\nu\overline{\nu}\nu$ final states, respectively. We expect about 2000 detected events in the muon channel, and 2400 in the electron channel per year of running. Including other 1-prong decays of the τ ($\pi\nu$ and $\rho\nu$) could increase the number of signal events by another 3000. But the background level for these channels will be much higher without the lepton identification cut. The main

source of the systematic error in the $\tau\nu$ measurement is the background subtraction, due to the uncertainty in D_s decay model. But at a Tau-Charm Factory, we will be able to complete the D_s model by measuring branching ratios with the tag sample.

Charged Higgs particle with a mass near D_s mass will enhance the $\tau\nu$ rate over $\mu\nu$. Fig. 4 shows the ratio of $B(D_s \to \mu\nu)/B(D_s \to \tau\nu)$ as a function of the Higgs mass. (We have divided out the factor coming from the W-propagator contribution, so that the ratio goes to unity in the absence of the Higgs.) If the Higgs mass is less than 3.5 GeV, it will be probably observed at a Tau-Charm Factory. As the Higgs mass becomes large, the sensitivity decreases, and above 4 GeV Higgs particle contribution becomes miniscule.

A similar plot can be drawn for the $D^+ \to \tau^+\nu$ decay, but it is very difficult to observe this decay because of the small branching ratio and large background rate. Due to the small phase space available, the branching fraction is around 5×10^{-4}, even though there is no helicity suppression. As in the case of $D_s^+ \to \tau^+\nu$, the main source of background is the decay channel, $K_L^0\mu^+(e^+)\nu$, which has a large branching fraction of 7 %, since it is not Cabibbo-suppressed in D^+ decay. We expect the background rate to be larger than the signal by an order of magnitude.

The leptonic decay of the B meson, $B^+ \to \tau^+\nu$, also has a small branching fraction of 5×10^{-5}, because of the small value of V_{ub}. Recent measurements[12] of $V_{ub}/V_{cb} = 0.10 \pm 0.03$ indicated that the value of V_{ub} is around 0.005. At a B-factory with luminosity of $10^{34}\ cm^{-2}sec^{-1}$, few $\times 10^5$ tagged B mesons are expected per year. With detection efficiency of $B^+ \to \tau^+\nu$ at the 20 % level, including the τ branching ratio, one expects a few detected $\tau\nu$ events against tags per year. While usage of partial tagging of the B, or an inclusive search for $\tau\nu$ could increase the efficiency by an order of magnitude, it would be at a cost of larger background, whose missing mass distribution is indistinguishable from the signal distribution itself.

SUMMARY

At a Tau-Charm Factory with a luminosity of $10^{33}\ cm^{-2}sec^{-1}$, weak decay constants of the D^+ and D_s^+ mesons will be measured with a precision of 1 % statistical error, using the decay D^+,$D_s^+ \rightarrow \mu^+\nu$. The weak decay constant of the B meson can be reliably extrapolated from this precision measurement. Lattice QCD calculations will mature by the time leptonic decays are measured at a Tau-Charm Factory, and calculation of weak decay constant will be a yardstick of the success of Lattice models. It will be also possible to observe the decay $D_s \rightarrow \tau\nu$. About 2000 events in $\mu\nu\bar{\nu}\nu$ final state and 2400 events in $e\nu\bar{\nu}\nu$ final state are expected per year. A search for charged Higgs of mass, $2 < M_H < 4$ GeV, can be made by comparing the observed $\tau\nu/\mu\nu$ ratio to the one expected from the W boson contribution.

REFERENCES

1. D. Bailin, *Weak Interactions*, Adam Hilger Ltd, Bristol (1982).
2. J. Adler *et al.*, Phys. Rev. Lett. **60**, 1375 (1988).
3. H. Krasemann, Phys. Lett 96B (1980) 397.
   E. Golowich, Phys. Lett. 91B (1980) 271.
   V. Mathur *et al.*, Phys. Lett. 107B (1981) 127.
   T. Aliev *et al.*, Sov. J. Nucl.Phys. 38 (1983) 6.
   M. Suzuki, Phys.Lett. 142B (1984) 207.
   S. Godfrey *et al.*, Phys. Rev. D32 (1985) 189.
   S. Godfrey, Phys. Rev. D33 (1986) 1391.
   C. Dominguez *et al.*, Phys. Lett. 197B (1987) 423.
   L. Reinders, Phys. Rev. D38 (1988) 947.
   C. Bernard *et al.*, Phys. Rev. D38 (1988) 3540.
   T. DeGrand *et al.*, Phys. Rev. D38 (1988) 954.
   N. Paver, Proceedings of the Tau-Charm Workshop, SLAC-REPORT 343.

4. W. Bartel *et al.,* Z. Phys. **C31**, 359 (1985).

5. Particle Data Group, Phys. Lett. **204**, 1 (1988).

6. C. H. Albright *et al.,* Phys. Rev. **D21**, 711 (1980).

7. M S. Alam (CLEO), presented at the 1989 International Symposium on Heavy Quark Physics, Cornell, June 1989.

8. A. S. Schwarz, Physica Scripta **33**, 5 (1986).

9. R. Schindler, Proceedings of the Tau-Charm Workshop, SLAC-REPORT 343.

10. J. Kirkby, *ibid.*

11. J. Adler *et al.,* Phys. Rev. Lett. **60**, 1375 (1988).
    J. Adler *et al.,* Phys. Rev. Lett. **62**, 1821 (1989).

12. M. Danilov (ARGUS) and D. Kreinick (CLEO), presented at the 24^{th} International Symposium on Lepton and Photon Interactions, Stanford, August 1989.

FIGURE CAPTIONS

1. D^+ or $D_s \to \mu\nu$ or $\tau\nu$.

2. (a) Missing mass for $D^+ \to \mu\nu$, shaded areas are backgrounds, (b) Missing mass for $D_s \to \mu\nu$, (c) Missing mass for $D_s \to \tau\nu$, $\tau \to \mu\bar{\nu}\nu$, and (d) Missing mass for $D_s \to \tau\nu$, $\tau \to e\bar{\nu}\nu$.

3. Missing mass distribution; shaded area are background with EM+HAD calorimeter veto, as shown in Fig. 2. Background shape with only EM calorimeter is also shown. (a) Missing mass for $D_s \to \tau\nu$, $\tau \to \mu\bar{\nu}\nu$ and (b) Missing mass for $D_s \to \tau\nu$, $\tau \to e\bar{\nu}\nu$.

4. Ratio between $\tau\nu$ and $\mu\nu$ rate in D_s decay as a unction of the Higgs mass. The dashed-line shows the expected statistical error on the ratio.

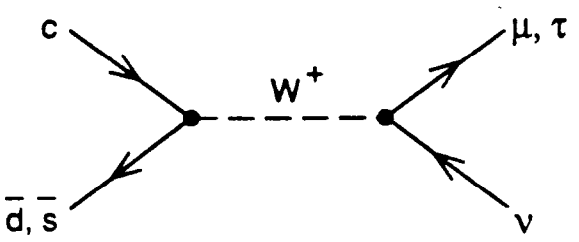

Figure 1

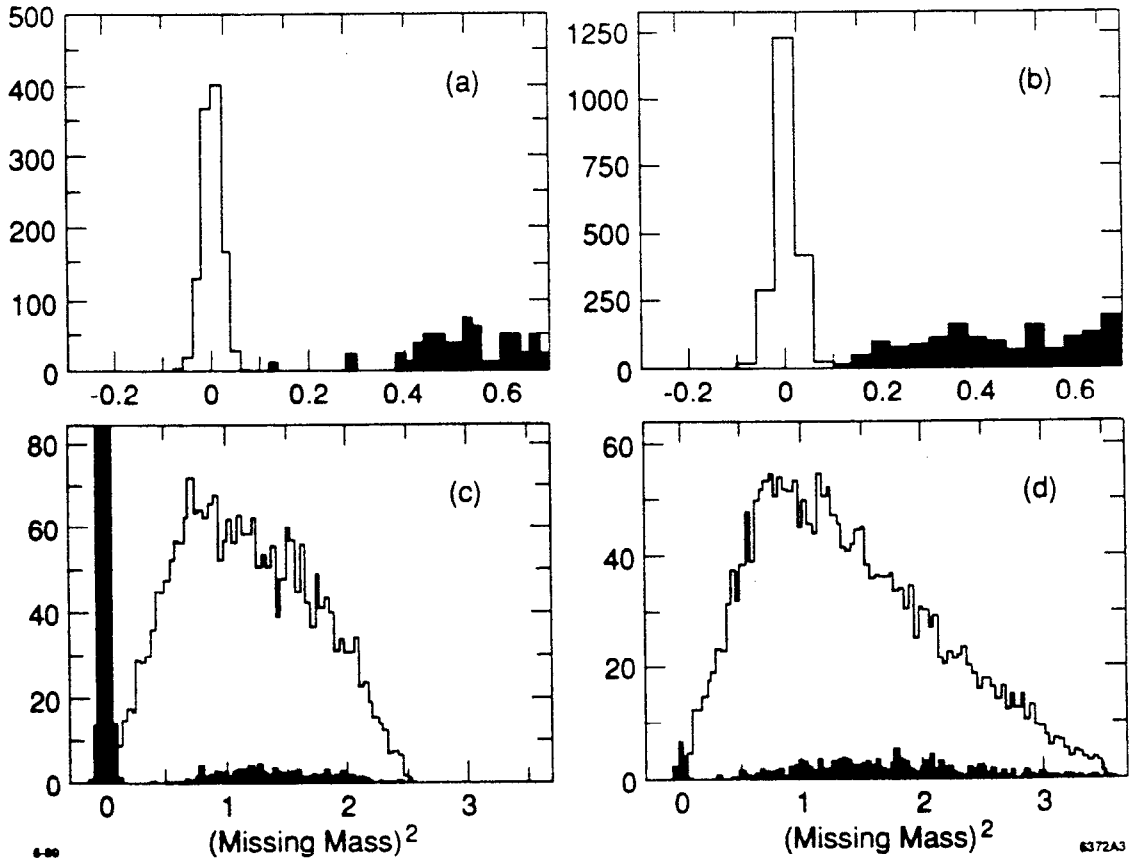

Figure 2

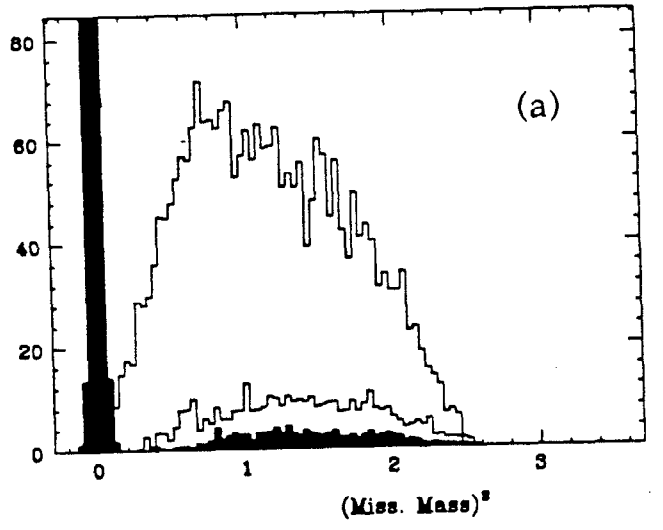

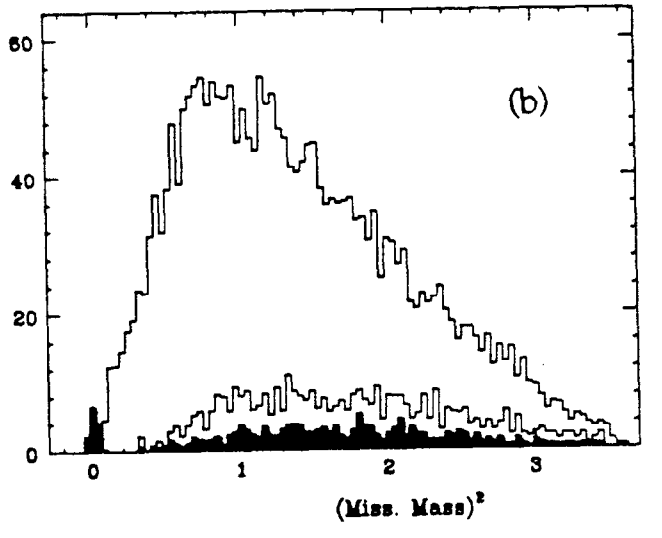

Figure 3

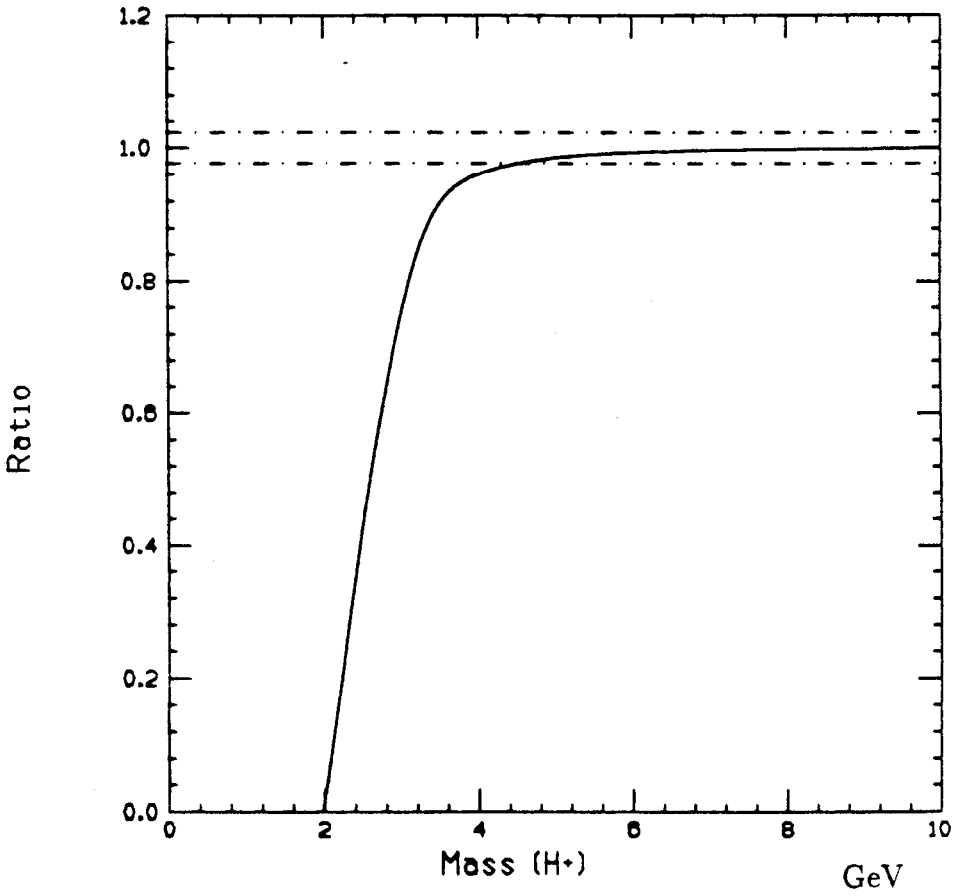

Figure 4